Natural Products

DOI: 10.1002/ange.201206658

Imaging Mass Spectrometry and Genome Mining Reveal Highly Antifungal Virulence Factor of Mushroom Soft Rot Pathogen**

*Katharina Graupner, Kirstin Scherlach, Tom Bretschneider, Gerald Lackner, Martin Roth, Harald Gross, and Christian Hertweck**

Soft rot diseases caused by a variety of bacteria account for severe losses in agriculture, devastating fruits, vegetables, and cultivated mushrooms. After bacterial infection, often owing to direct contact or transmission by insects, virulence factors and lytic enzymes cause degradation of plant and mushroom tissues, thereby turning crop into mush.[1–3] In many cases, the chemical mediators of soft rot diseases have remained elusive, as in the long-known mushroom pathogen *Janthinobacterium agaricidamnosum*.[4] This motile Gram-negative bacterium has been found to be the causative agent of soft rot disease of the cultured button mushroom, *Agaricus bisporus*. Typical symptoms of the infection are lesions turning into sticky blotches on the cap surface and a complete dissolution of the mushroom within only a few days (Figure 1 A, B).[4] We reasoned that knowledge on the causative agent of the soft rot would have a double benefit. Foremost, it could aid in understanding the pathobiology of the mushroom pathogen, which may be a starting point for protective measures. Second, there is an increasing need for novel antifungals, since the incidents of severe and even lethal fungal infections and resistance towards antifungals are on the rise.[5] We hypothesized that mushroom soft rot bacteria could excrete antifungal agents as virulence factors, which might also be active against human pathogens. Herein we report the discovery and full characterization of a highly antifungal virulence factor from the soft rot pathogen *Janthinobacterium agaricidamnosum* guided by imaging mass spectrometry and genome mining.

To gain insight into the metabolic potential of *J. agaricidamnosum*, we subjected genomic DNA of the bacterium to shotgun sequencing. Bioinformatic mining of the *J. agaricidamnosum* draft genome sequence revealed several gene loci,

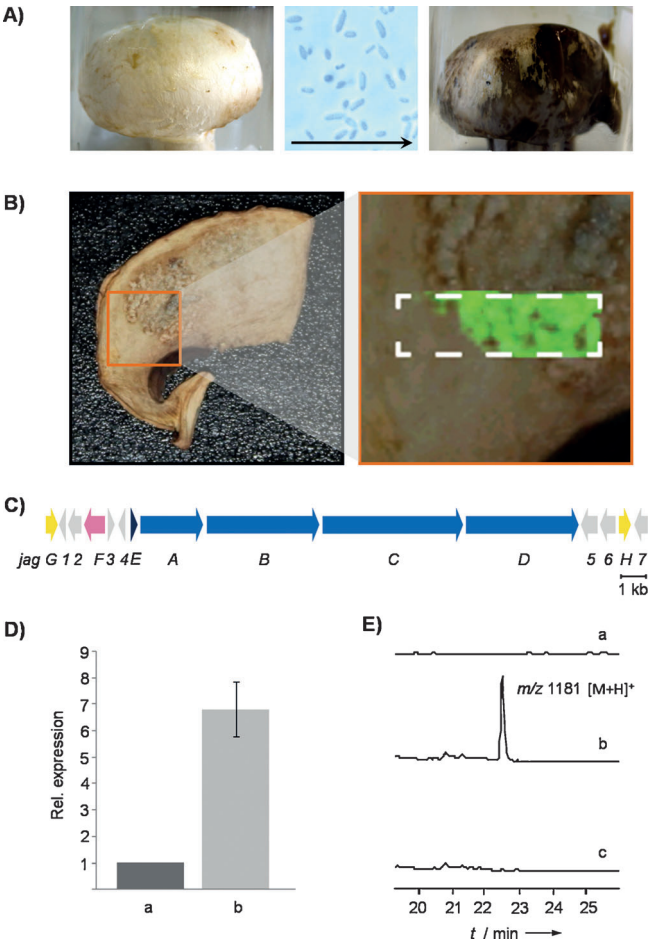

Figure 1. A) Pictures of button mushroom before and after (72 h) infection with *Janthinobacterium agaricidamnosum* (micrograph, center). B) Imaging mass spectrometry of a mushroom fruiting body inoculated with *J. agaricidamnosum*; dried mushroom slice showing bacteria-induced lesion (left), enlarged view of the lesion and imaging area (right). The dashed area was laser-scanned with a raster width of 100 µm. The occurrence of the ion $[M+H]^+$ 1181 (for jagaricin) is visualized in green. C) Architecture of the *jag* biosynthesis gene locus (GenBank accession nr. HE967328); NRPS and accessory genes (blue and black), regulator genes (yellow), transporter gene (pink), other (gray). D) RTq-PCR expression analysis of NRPS gene *jagA*; a) non-producing conditions, b) producing conditions. E) HPLC profiles of wild-type *J. agaricidamnosum* in standard growth medium (a), same in modified production medium (b), Δ*jagA* mutant (c).

[*] K. Graupner, Dr. K. Scherlach, T. Bretschneider, Dr. G. Lackner, Dr. M. Roth, Prof. Dr. C. Hertweck
Department of Biomolecular Chemistry
Leibniz Institute for Natural Product Research and Infection Biology, HKI
Beutenbergstrasse 11a, 07745 Jena (Germany)
E-mail: christian.hertweck@hki-jena.de
Prof. Dr. H. Gross
Eberhard Karls University, Tübingen (Germany)
Prof. Dr. C. Hertweck
Friedrich Schiller University, Jena (Germany)

[**] We thank A. Perner, F. Rhein, and H. Heinecke for MS and NMR measurements, N. Ueberschaar for GC-MS, M.-G. Schwinger, M. Ishida, C. Weigel, and H.-M. Dahse for bioactivity testing, G. Krauter, J. Schönemann, K. Willing, and M.-G. Schwinger for fermentations. We are grateful for financial support by the Pakt für Forschung und Innovation and the ILRS as part of the excellence graduate school Jena School for Microbial Communication (JSMC).

Supporting information for this article is available on the WWW under http://dx.doi.org/10.1002/anie.201206658.

such as the *jag* gene locus (Figure 1C), that code for thiotemplate systems composed of modular polyketide synthase (PKS) and nonribosomal peptide synthetase (NRPS) modules. Thus, the mushroom pathogen would in principle have the capacity to produce complex secondary metabolites. Nonetheless, by quantitative reverse-transcriptase PCR (RTq-PCR) we found that the PKS and NRPS gene loci are silent or downregulated under standard cultivation conditions (Figure 1D). This is in line with the observation that *J. agaricidamnosum* grown under these conditions does not produce any secondary metabolites (Figure 1E, lane a). Apparently, the production of these cryptic natural products requires a particular trigger,[6] and thus we aimed at catching the pathogen in action while infecting a mushroom fruiting body.

For this purpose imaging mass spectrometry appeared to be a promising method.[7,8] First, we inoculated slices of *Agaricus bisporus* with *J. agaricidamnosum* and monitored the formation of bacteria-induced tissue lesions. Next, a liquid matrix containing α-cyano-4-hydroxy cinnamic acid was sprayed onto the surface of the infected mushroom. The imaging area was automatically scanned with a raster width of 100 μm in XY recording 1000 spectra at each spot with a laser frequency of 1000 Hz. MALDI-MS measurements were performed using an ultrafleXtreme mass spectrometer in the positive reflector mode collecting data in the range of m/z 900–2000 Da. The resultant sum spectrum was evaluated manually, and the mass of interest was visualized in the logarithmic scale by picking the peak with 1 Da mass range using the brightness optimization as implemented in flexImaging. In this way we visualized the production of a new compound with m/z 1181 $[M+H]^+$ within the damaged mushroom tissue (Figure 1B). We next aimed at stimulating the formation of the metabolite in liquid media. From a variety of media screened we found that traces of the new compound were produced in minimal medium containing mushroom cubes. Higher yields were, however, obtained using a complex culture medium (5 g L^{-1} glycine, 10 g L^{-1} yeast extract, 10 g L^{-1} glucose, 10 g L^{-1} corn steep, 10 g L^{-1} $CaCO_3$), which also proved to be more convenient when increasing the culture volume. From high-resolution mass spectrometry measurements (Exactive, Thermo Scientific) we inferred the elementary composition of $C_{56}H_{85}N_{12}O_{16}$ for the new metabolite, named jagaricin. Considering the size and elementary composition of the molecule, we assumed that the corresponding gene cluster would harbor NRPS genes. The best candidate for mediating jagaricin biosynthesis would be the *jag* gene locus (Figure 1C), since the size of the putative product of the encoded synthase is similar to jagaricin. RTq-PCR measurements confirmed that the *jag* genes were substantially upregulated under these producing conditions (Figure 1D). Open reading frames (orfs) *jagA–H* code for a nonamodular NRPS (*jag*A–D) as well as several accessory and regulatory components (*jagE–H*). By employing the modular structure of the encoded NRPS, the adenylation (A) domain specificities inferred in silico (see the Supporting Information), and MS/MS analyses we predicted that jagaricin is a cyclic lipopeptide with the amino acid sequence Dhb-Thr-Thr-Tyr-Dhb-Gln-Gly-Thr-His (Dhb, dehydrobutyrine) and an N-terminal acyl residue ($C_{14}H_{26}O_2$).

To obtain a sufficient amount of jagaricin for a full structural characterization and biological evaluation, the fermentation was upscaled to 50 L. Size exclusion chromatography followed by repeated preparative RP-HPLC yielded 29 mg of pure jagaricin. 1D and 2D NMR studies confirmed the architecture of the jagaricin peptide backbone that was predicted by MS^n and bioinformatics analyses (Figure 2A). NMR spectroscopy data also revealed that the N-terminal acyl moiety is derived from β-hydroxymyristic acid (HMA). The absolute configuration of HMA obtained by acid hydrolysis of jagaricin was determined to be *R* in the 3-position of HMA by employing GC–MS analysis of the corresponding Mosher ester and authentic (*R*)- and (*S*)-HMA

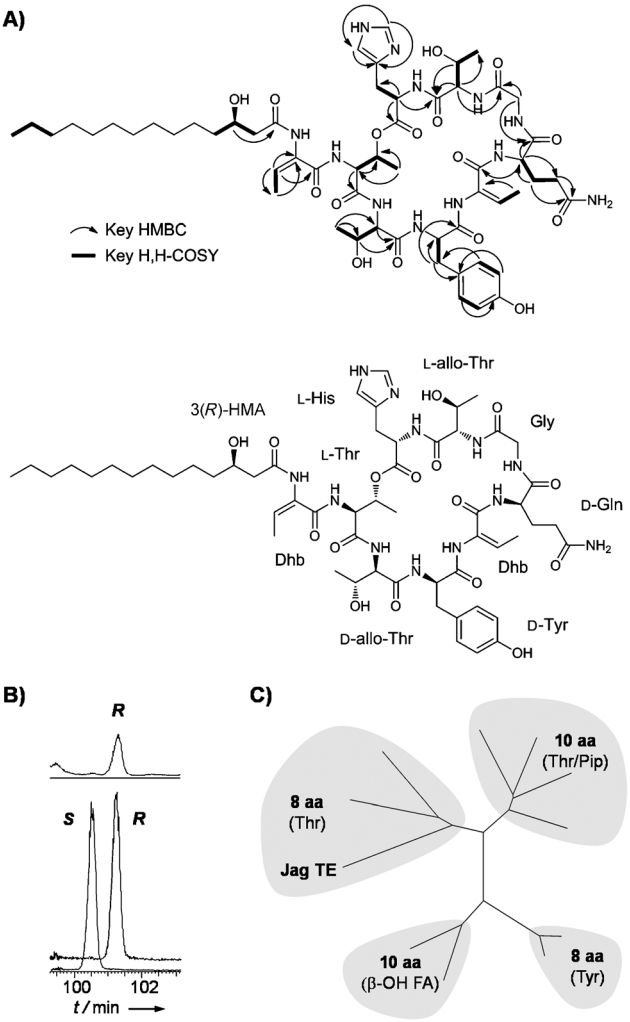

Figure 2. Full structure elucidation of jagaricin. A) Key results from 2D NMR spectroscopy, degradation experiments, and application of Marfey's method. B) Stereochemical elucidation of HMA (as Mosher ester) by GC–MS analysis and comparison with equally derivatized (*R*)- and (*S*)-HMA references (lower traces); C) Phylogeny of TE domains to deduce connectivity and lactone ring size of jagaricin; the ring size of the cyclopeptide (number of aa) and the molecule where the formation of the ester bond occurs are shown; β-OH FA = hydroxy fatty acid; Pip = pipecolin.

references (Figure 2B). The absolute configurations of the free amino acids were elucidated by derivatization with Marfey's reagent and HPLC analyses using 1-fluoro-2,4-dinitrophenyl-5-L-alanine-amide (L-FDAA) conjugates of D- and L-amino acids as references (see the Supporting Information).

Whereas the architecture and absolute configuration of the lipopeptide backbone could be rigorously determined by means of NMR spectroscopy, MS^n, and chemical degradation, the position of the ester bond remained ambiguous. Several Thr residues could in principle provide the hydroxy residue, yet no diagnostic couplings were observed by 2D NMR spectroscopy. For this reason we performed a phylogenetic analysis of thioesterase (TE) domains from various NRPSs producing cyclopeptides of different ring sizes. In the cladogram the *jag* TE falls into a clade of TEs producing cyclooctapeptides (Figure 2C). We thus concluded that the ester bond is located between the His carboxy group and the hydroxy moiety of the first Thr residue. To corroborate this, we peracetylated jagaricin, and indeed NMR data of *O*-acetylated jagaricin were in full agreement with the predicted position of the ring closure (see the Supporting Information).

We have thus fully elucidated the structure of jagaricin, a novel lipopeptide containing two Dhb residues that are rather uncommon for NRPS products. Actually, these enamino acids are a hallmark of ribosomally produced lantibiotics, where they mainly occur as precursors of the lanthionine building blocks.[9] In contrast, the mechanism and timing of Dhb formation in NRPS-derived peptides is still unknown. Overall, the structure of jagaricin correlates well with the encoded NRPS assembly line (Figure 3). However, the jagaricin synthetase has some interesting features that breach with canonical NRPS functions.[10,11] First, an A domain is clearly missing in module 2. Considering the Thr specificity of the upstream A domain, it is well conceivable that it loads the second Thr residue, too. This scenario would be reminiscent of the yersiniabactin synthetase, where a single A domain in the second module loads cysteine units onto two individual downstream T domains.[12,13] Next, the stereochemical analysis showed unequivocally that D-Tyr is incorporated into the peptide chain, yet no epimerization domain can be found in module 4 (Figure 3). A detailed analysis of the C domain in the downstream module revealed the signature sequences of a $^{D}C_{L}$ domain, which is known to link an L-amino acid to a D-amino acid.[14] Hence, the upstream A domain seems to activate D-Tyr, which is likely generated by a racemase. Notably, there is only a small number of known pathways where D-amino acids are incorporated into NRPs by this mechanism.[15–18] Another surprising finding was that module 8 possesses an additional C domain. It has been suggested that the second C domain catalyzes the epimerization of the Thr side chain, thereby leading to the insertion of L-allo-Thr into the growing peptide chain.[19] The fact that L-allo-Thr is incorporated by the *jag* NRPS at this particular position supports this prediction. Remarkably, only two NRPSs are known that harbor the same unusual domain structure.[19,20]

The expression studies and the clear correlation of structure and NRPS architecture already indicate a link between the *jag* gene locus and the production of jagaricin. However, for a rigorous assignment a gene knockout was essential. To achieve this goal proved to be most challenging, since neither genetic tools nor protocols were available for this extraordinary bacterium. Eventually, we succeeded in transforming *J. agaricidamnosum* and disrupting the NRPS gene *jagA* by insertion of a kanamycin resistance cassette. The

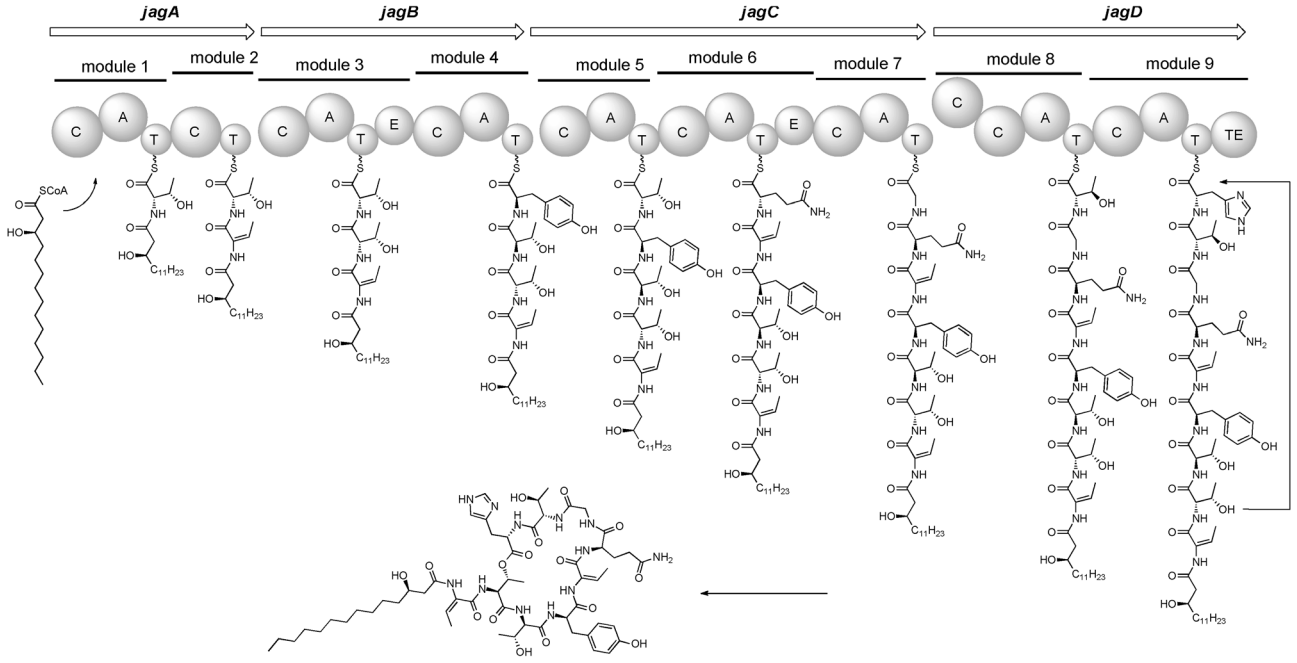

Figure 3. Deduced NRPS thiotemplate and model for the biosynthesis of jagaricin. The timing of Dhb formation from Thr is approximate. C = condensation domain; A = adenylation domain; T = thiolation domain; E = epimerization domain; TE = thioesterase domain.

successful mutant construction was confirmed by PCR, and indeed the jagaricin formation was completely abrogated in the Δ*jagA* mutant (Figure 1E, lane c). Thus, the identity of the *jag* gene cluster was unequivocally confirmed. Moreover, when growing the Δ*jag*A mutant on mushroom tissue, no jagaricin could be detected by imaging MS. To further corroborate the role of jagaricin in the infection process we applied pure jagaricin onto mushroom tissue. We noted that the lipopeptide alone caused a superficial lesion that is symptomatic to the wild type of the soft rot pathogen (Figure 4A). These results indicate that jagaricin is clearly

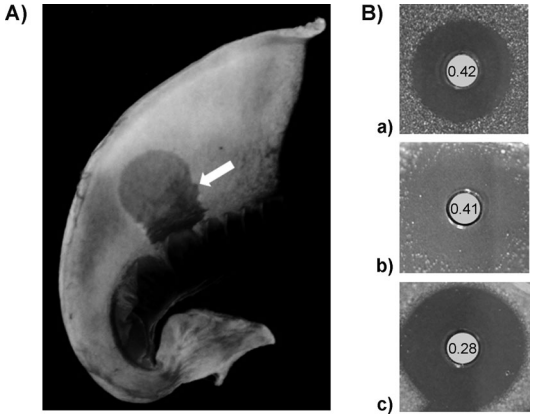

Figure 4. Biological evaluation of jagaricin. A) Induction of mushroom tissue lesions with pure jagaricin solution. The arrow indicates the position of the lesion. B) Antifungal activity of jagaricin against a) *Candida albicans*, b) *Aspergillus fumigatus*, c) *Aspergillus terreus* (agar diffusion assay with $c = 500\ \mu g\,mL^{-1}$); minimal inhibitory concentration (MIC_{100}) values in μM.

involved in the infection process. However, jagaricin is apparently not the only pathogenicity factor, as enzymes such as chitinases may contribute to the further degradation of the fruiting bodies. This finding is interesting in light of the other known mechanisms of mushroom pathogens. Investigation of brown blotch disease caused by *Pseudomonas* spp. revealed tolaasin as the sole virulence factor,[21] whereas degradative enzymes have been shown to be the only virulence factor in the cavity disease caused by *Burkholderia gladioli* pv. agaricicola.[22] An analogous case where secondary metabolites are not the only determinants for pathogenicity but support infection has been described for the plant pathogen *Pseudomonas syringae*.[23]

Since jagaricin exerts a clear antifungal effect on the mushroom, we next tested our hypothesis that the virulence factor may also act as an agent against pathogenic fungi. For this purpose jagaricin was subjected to an antimicrobial profiling. By using a panel of representative test strains we found that jagaricin has only little or no antibacterial activity. In contrast, the lipopeptide is highly active against the major human pathogens *Candida albicans*, *Aspergillus fumigatus*, and *Aspergillus terreus* even at submicromolar concentrations (Figure 4B). At 3–10x higher concentrations jagaricin exhibits antiproliferative and cytotoxic activity (see the Supporting Information). Taken together, this finding is a proof of concept that the elucidation of virulence factors involved in mushroom diseases may lead to the discovery of natural products that are also active against human pathogenic fungi. Further biological evaluations will reveal possible applications of jagaricin as a therapeutic.

Herein we have reported the discovery of a new antifungal virulence factor, jagaricin, the discovery of which proved to be challenging, because the *jag* biosynthesis genes are downregulated or silenced under regular cultivation conditions. In the pathobiological context jagaricin production is triggered upon contact of the bacterium (*J. agaricidamnosum*) with the mushroom (*A. bisporus*). To elucidate the cryptic natural product we employed a combination of imaging mass spectrometry and genome mining. Imaging mass spectrometry has proven to be a valuable tool for the discovery of microbial and plant natural products, in particular in symbioses.[24–26] Coupling this technique to genome mining is a new approach,[27–29] and to our knowledge we describe the first case where this combination enabled the systematic discovery and full characterization of a cryptic natural product. Furthermore, the revelation of a virulence factor by imaging mass spectrometry and genomics is unprecedented. For the rigorous elucidation of the antifungal principle the combination of physicochemical methods, chemical derivatization, and bioinformatics analysis of the encoded NRPS assembly line was most effective. Herein, predicting the lactone ring size by a TE phylogeny proved to be a particularly valuable, new approach that will certainly aid in solving related structural riddles. Furthermore, comparison of the jagaricin structure and the thiotemplate system revealed several unusual features of the *jag* NRPS. In this regard it should be highlighted that the identity of the *jag* biosynthesis gene locus was unequivocally proven by a gene knockout, which proved to be challenging considering that this unusual bacterium has been genetically fully unexplored. On ecological and agricultural grounds the discovery of the virulence factor and the corresponding genes is significant, because it helps understanding the pathobiology of bacteria-induced soft rot. From a chemical point of view, our study highlights the impact of blending modern analytics with genetics to unveil cryptic natural products from neglected microorganisms.[30] The general approach of combining imaging mass spectrometry with genome mining holds promise to be generally applicable to the discovery of cryptic natural products including chemical mediators such as virulence factors that are only produced in a particular (patho)biological context.

Received: August 17, 2012
Revised: October 22, 2012
Published online: November 19, 2012

Keywords: biosynthesis · natural products · *Janthinobacterium agaricidamnosum* · lipopeptides · structure elucidation

[1] M. L. Largeteau, J. M. Savoie, *Appl. Microbiol. Biotechnol.* **2010**, *86*, 63.

[2] A. O. Charkowski, *Curr. Opin. Biotechnol.* **2009**, *20*, 178.
[3] D. Y. Kobayashi, J. A. Crouch, *Annu. Rev. Phytopathol.* **2009**, *47*, 63.
[4] S. P. Lincoln, T. R. Fermor, B. J. Tindall, *Int. J. Syst. Bacteriol.* **1999**, *49*, 1577.
[5] R. Di Santo, *Nat. Prod. Rep.* **2010**, *27*, 1084.
[6] K. Scherlach, C. Hertweck, *Org. Biomol. Chem.* **2009**, *7*, 1753.
[7] A. Svatoš, *Trends Biotechnol.* **2010**, *28*, 425.
[8] E. Esquenazi, Y. L. Yang, J. Watrous, W. H. Gerwick, P. C. Dorrestein, *Nat. Prod. Rep.* **2009**, *26*, 1521.
[9] J. M. Willey, W. A. van der Donk, *Annu. Rev. Microbiol.* **2007**, *61*, 477.
[10] D. Schwarzer, R. Finking, M. A. Marahiel, *Nat. Prod. Rep.* **2003**, *20*, 275.
[11] H. L. Condurso, S. D. Bruner, *Nat. Prod. Rep.* **2012**, *29*, 1099 – 1110.
[12] A. M. Gehring, E. DeMoll, J. D. Fetherston, I. Mori, G. F. Mayhew, F. R. Blattner, C. T. Walsh, R. D. Perry, *Chem. Biol.* **1998**, *5*, 573.
[13] Z. Suo, C. T. Walsh, D. A. Miller, *Biochemistry* **1999**, *38*, 14023.
[14] C. Rausch, I. Hoof, T. Weber, W. Wohlleben, D. H. Huson, *BMC Evol. Biol.* **2007**, *7*, 78.
[15] G. Weber, K. Schörgendorfer, E. Schneider-Scherzer, E. Leitner, *Curr. Genet.* **1994**, *26*, 120.
[16] D. Tillett, E. Dittmann, M. Erhard, H. von Döhren, T. Börner, B. A. Neilan, *Chem. Biol.* **2000**, *7*, 753.
[17] Y. Q. Cheng, J. D. Walton, *J. Biol. Chem.* **2000**, *275*, 4906.
[18] K. Ishida, T. Lincke, C. Hertweck, *Angew. Chem.* **2012**, *124*, 5566 – 5570; *Angew. Chem. Int. Ed.* **2012**, *51*, 5470 – 5474.
[19] J. Hou, L. Robbel, M. A. Marahiel, *Chem. Biol.* **2011**, *18*, 655.
[20] R. Mendes, M. Kruijt, I. de Bruijn, E. Dekkers, M. van der Voort, J. H. Schneider, Y. M. Piceno, T. Z. DeSantis, G. L. Andersen, P. A. Bakker, J. M. Raaijmakers, *Science* **2011**, *332*, 1097.
[21] C. Soler-Rivas, S. Jolivet, N. Arpin, J. M. Olivier, H. J. Wichers, *FEMS Microbiol. Rev.* **1999**, *23*, 591.
[22] P. Roy Chowdhury, J. A. Heinemann, *Appl. Environ. Microbiol.* **2006**, *72*, 3558.
[23] C. L. Bender, F. Alarcón-Chaidez, D. C. Gross, *Microbiol. Mol. Biol. Rev.* **1999**, *63*, 266.
[24] J. Kroiss, M. Kaltenpoth, B. Schneider, M. G. Schwinger, C. Hertweck, R. K. Maddula, E. Strohm, A. Svatos, *Nat. Chem. Biol.* **2010**, *6*, 261.
[25] I. Schoenian, M. Spiteller, M. Ghaste, R. Wirth, H. Herz, D. Spiteller, *Proc. Natl. Acad. Sci. USA* **2011**, *108*, 1955.
[26] Y. L. Yang, Y. Xu, R. D. Kersten, W. T. Liu, M. J. Meehan, B. S. Moore, N. Bandeira, P. C. Dorrestein, *Angew. Chem.* **2011**, *123*, 5961; *Angew. Chem. Int. Ed.* **2011**, *50*, 5839.
[27] R. D. Kersten, Y. L. Yang, Y. Xu, P. Cimermancic, S. J. Nam, W. Fenical, M. A. Fischbach, B. S. Moore, P. C. Dorrestein, *Nat. Chem. Biol.* **2011**, *7*, 794.
[28] W. T. Liu, R. D. Kersten, Y. L. Yang, B. S. Moore, P. C. Dorrestein, *J. Am. Chem. Soc.* **2011**, *133*, 18010.
[29] J. Watrous, P. Roach, T. Alexandrov, B. S. Heath, J. Y. Yang, R. D. Kersten, M. van der Voort, K. Pogliano, H. Gross, J. M. Raaijmakers, B. S. Moore, J. Laskin, N. Bandeira, P. C. Dorrestein, *Proc. Natl. Acad. Sci. USA* **2012**, *109*, E1743.
[30] J. M. Winter, S. Behnken, C. Hertweck, *Curr. Opin. Chem. Biol.* **2011**, *15*, 22.

